Science Bulletin 64 (2019) 108–121

Contents lists available at ScienceDirect

Science Bulletin

journal homepage: www.elsevier.com/locate/scib

Article

Distinctive melt activity and chromite mineralization in Luobusa and Purang ophiolites, southern Tibet: constraints from trace element compositions of chromite and olivine

Benxun Su [a,b,c,*], Meifu Zhou [d], Jiejun Jing [a,b,c], Paul T. Robinson [a,d], Chen Chen [a,b,c], Yan Xiao [c,e], Xia Liu [a,b,c], Rendeng Shi [f], Davide Lenaz [g], Yan Hu [h]

[a] Key Laboratory of Mineral Resources, Institute of Geology and Geophysics, Chinese Academy of Sciences, Beijing 100029, China
[b] University of Chinese Academy of Sciences, Beijing 100049, China
[c] Institutions of Earth Science, Chinese Academy of Sciences, Beijing 100029, China
[d] Department of Earth Sciences, The University of Hong Kong, Hong Kong, China
[e] State Key Laboratory of Lithospheric Evolution, Institute of Geology and Geophysics, Chinese Academy of Sciences, Beijing 100029, China
[f] Key Laboratory of Continental Collision and Plateau Uplift, Institute of Tibetan Plateau Research, Chinese Academy of Sciences, Beijing 100101, China
[g] Department of Mathematics and Geosciences, University of Trieste, Via Weiss 8, Trieste 34127, Italy
[h] Department of Earth and Space Sciences, University of Washington, Seattle, WA 98195, USA

ARTICLE INFO

Article history:
Received 16 October 2018
Received in revised form 16 December 2018
Accepted 17 December 2018
Available online 22 December 2018

Keywords:
Chromite
Olivine
Ophiolite
Trace element
Tibet

ABSTRACT

To investigate the factors controlling the mineralization in ophiolites we systematically compared the petrology and mineral compositions of the harzburgites/lherzolites, dunites and chromitites in the Luobusa and Purang ophiolites. Generally, the petrological features and trace element compositions of chromite and olivine in peridotite and chromitite are distinctly different between the two ophiolites. In Luobusa, boninitic melts are inferred to have interacted with the harzburgites and modified the distributions of some trace elements (e.g., Ni, Mn and V) in chromite and olivine. The subsequently formed dunites and chromitites experienced significant elemental exchange. In contrast, the Purang ophiolite contains a wider range of chromitite compositions and records diverse melt activities, such as the growth of relatively abundant secondary clinopyroxene. The metasomatic melts were enriched in Al and depleted in Si, Na and highly incompatible trace elements (e.g., Nb, Zr). Such melts resemble MORB-like melts proposed in the literature but are assumed to be more hydrous than typical MORB because of presence of hydrous minerals. The parental magmas of the Purang dunites and intermediate chromitites are inferred to be compositionally intermediate between boninitic and MORB-like melts. In addition, the more refractory nature of the Luobusa harzburgites facilitated a high Cr concentration gradient with the interacting melts, making it easier to increase Cr in the melts. Crystallization of clinopyroxene and amphibole in the Purang ophiolite accommodated significant amounts of Cr and water, respectively, and negatively affected Cr concentration and chromite crystallization. The concentration of chromite to form chromitites requires the presence of focused melt channels.

1. Introduction

Most ophiolites, from their generation in an ocean to emplacement on land, would experience extensive melt invasion and consequent lithological and compositional modification [1–4]. Melt-peridotite interaction has been genetically linked to the formation of chromite deposits in ophiolites [5–8], but there is no consensus on the factors that determine whether a given ophiolite is mineralized or barren [9–11]. Chromite deposits in ophiolites are typically hosted in harzburgites where they are surrounded by dunite envelopes that grade outward into the peridotites [12–15]. These three lithologies typically have simple mineral assemblages composed chiefly of olivine and magnesiochromite (chromite hereafter) accompanied by orthopyroxene and locally by minor amounts of clinopyroxene. Both olivine and chromite have relatively simple compositions but typically contain detectable trace elements and radiogenic isotopes [16,17]. In most previous studies, melt compositions were constrained by comparing major oxide compositions of chromite with those in associated

* Corresponding author.
E-mail address: subenxun@mail.iggcas.ac.cn (B. Su).

https://doi.org/10.1016/j.scib.2018.12.018
2095-9273/

magmatic rocks [15,18–21]. These studies proposed that high-Al and high-Cr chromitites are formed from MORB-like and boninitic melts, respectively [8,15,22]. Nonetheless, olivine coexisting with chromite are not comparable in composition [17].

Olivine and chromite can crystallize as early phases from mafic magmas and can be residual phases after partial melting of mantle peridotites [18,23,24]. They are thus traditionally thought to be important petrogenetic indicators [25–27], particularly chromite, which is more resistant to alteration and weathering than olivine. Recently, some authors have used trace elements and Li, Mg and Fe isotopes to gain new insights into the genesis of chromite deposits [4,10,16,28–32] and have shown that such elements can be used as indices of partial melting, fractional crystallization, melt-rock interaction and chemical diffusion [10,21,32–34]. Incompatible trace elements in olivine and chromite are sensitive to melting and differentiation processes, whereas compatible trace elements are mostly used to identify source compositions [35,36].

Although the study of trace element compositions of olivine and chromite has increased in recent years [10,21,37–43], the application of these data to understand chromite mineralization in ophiolite is still in an early stage. To our knowledge there are, as yet, no comprehensive studies on trace element compositions of olivine and chromite in chromitites or their host peridotites.

Here we provide in situ trace element analyses of olivine and chromite in chromitites and peridotites from the chromite deposit-bearing Luobusa and barren Purang ophiolites in the Yarlung Zangbo Suture Zone of southern Tibet. These datasets, together with petrological investigations and mineral major oxide compositions, are used to constrain melt activity and its relation to the formation of chromite deposit. Elemental compositions between the two massifs are systematically compared to identify potential chemical proxies for chromite mineralization in ophiolites.

2. Geology of the Purang and Luobusa ophiolites

The Tibetan Plateau consists of several major blocks, which were welded successively to the Eurasian continent along successive suture zones [3] (Fig. 1a). The Yarlung Zangbo Suture Zone, the southernmost and youngest, marks the final collision between the Indian block and the Eurasian plate [44,45]. This suture zone, which extends ~2,000 km from east to west, contains numerous Cretaceous ophiolites (Fig. 1b) that represent remnants of the Neo-Tethyan oceanic lithosphere [46,47]. The Purang (Fig. 1c) and Luobusa (Fig. 1d) ophiolites are located in the western and eastern parts of the Yarlung Zangbo Suture Zone, respectively. Most of the ophiolites in the Yarlung Zangbo Suture, including Purang, lack significant podiform chromitites, whereas the Luobusa ophiolite hosts the largest chromite deposit in China [48].

2.1. Purang ophiolite

The Purang ophiolite outcrops over an area of ~800 km^2 in westernmost Tibet and consists chiefly of a large ultramafic massif with minor crustal rocks (Fig. 1c). The ultramafic massif is dominated by harzburgite with yellowish-brown weathering surfaces (Fig. 2a), but subordinate lherzolite occurs as massive bodies in the northern part of the ophiolite and as small lenses randomly distributed in the harzburgite [49–51] (Fig. 1c). Minor chromitite

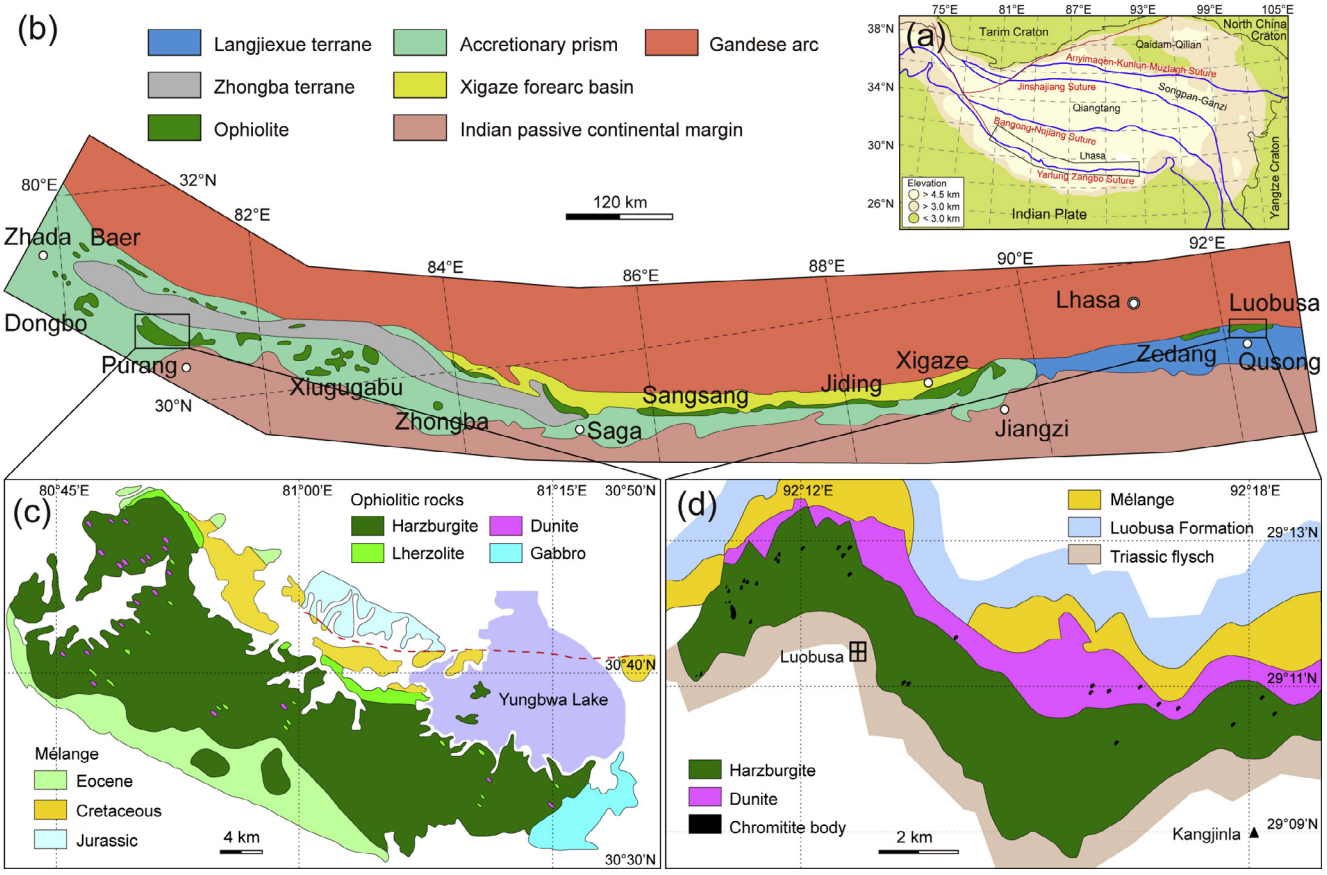

Fig. 1. Geology map of the study area. (a) Sketch tectonic map of Tibetan Plateau showing its major sutures. (b) Distribution of ophiolites in Yarlung Zangbo Suture Zone in southern Tibet. (c) Geologic map of Purang ophiolite. (d) Geologic map of Luobusa ophiolite.

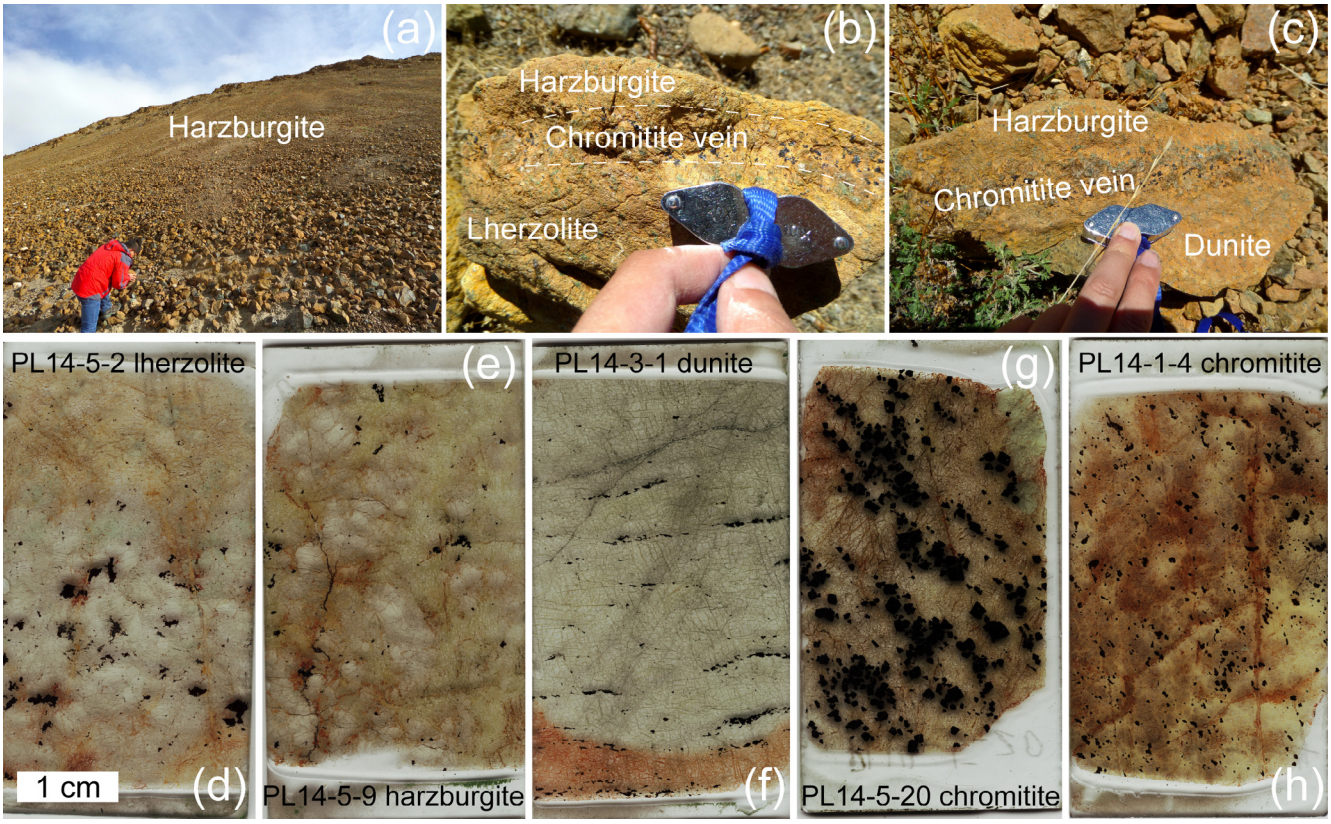

Fig. 2. Occurrence of rocks from the Purang ophiolite (a–c) and scanned images of thin sections (d–h).

veins commonly occur along the contact between the harzburgites and lherzolites (Fig. 2b) or dunites (Fig. 2c). Some chromitite bodies, with ore types ranging from disseminated to massive chromitite, are locally enveloped in dunite in the host harzburgite [52–54].

Once the weathered surfaces are removed, most samples are fresh and have well-defined grain boundaries in thin section [29,49] (Fig. 3d–g), however, olivine in some chromitite samples is variably altered [53] (Fig. 3h).

Mafic rocks of the crustal section mostly form a massive body in the eastern part of the ophiolite (Fig. 1c), but mafic dykes and veins are also scattered in the harzburgites [54–56]. In addition, pyroxenite veins are also common in the harzburgite massif [50]. Diabase dykes have zircon U-Pb ages of ca. 120 Ma [57,58], and gabbro dykes have ages of 130 Ma [59] and ca. 124 Ma [60]. Geochemically, these mafic rocks have an affinity with normal mid-ocean ridge basalt (N-MORB) [29,54,55].

2.2. Luobusa ophiolite

The Luobusa ophiolite lies about 200 km east-southeast of Lhasa city (Fig. 1b). It is a tectonically bounded slice, at least 3 km thick, and has been thrust northward onto the Tertiary molasse deposits of the Luobusa Formation and the Gangdese batholiths. To the south, it is separated from Triassic flysch deposits by a steep reverse fault [16,48] (Fig. 1d). The base of the ophiolite is marked by a tectonic mélange containing blocks of pillow lavas and cumulate rocks, including wehrlite, pyroxenite, and layered and homogeneous gabbros, in a highly serpentinized ultramafic matrix. Geochronological studies have yielded variable ages ranging from 177 Ma [61] to 163 Ma [62] and ca. 150 Ma [60] for diabase, and ca. 130 Ma [63] and 150 Ma [60] for gabbro. Malpas et al. [45] suggested that the range of ages represented a two-stage origin for the ophiolite.

The Luobusa ophiolite consists chiefly of mantle harzburgite and clinopyroxene-bearing harzburgite with abundant lenses and pods of dunite and chromitite, structurally underlain by a layer of transition zone dunite [15,64,65] (Fig. 1d). The transition zone sequence contains a few seams and pods of chromitite up to several meters thick, but the major podiform chromitites are all hosted in the harzburgites. Individual chromitites are typically lens shaped, although many occur as large, massive blocks and tabular or pencil-like bodies [66]. Typical chromitite bodies range from 20 to 250 m long, 10 to 100 m wide and 0 to 5 m thick and have an average grade of 48 wt% Cr_2O_3 [48,67], which places them in the metallurgic category. Most of the bodies are hosted in harzburgite, although minor deposits also occur in the clinopyroxene-bearing harzburgite along the southern margin of the ophiolite [67]. Most of the chromitite orebodies occur in a narrow band, generally 500–600 m structurally below the crust-mantle transition zone, where they are typically enclosed in dunite or have dunite envelopes several centimeters to several meters thick. These envelopes grade outward into the surrounding harzburgite or clinopyroxene-bearing harzburgite with increasing modal proportions of pyroxene [15,30,68], and their thickness is independent of the size of the chromitite body. Massive, disseminated, nodular, anti-nodular and brecciated chromitites are the most common textural types and these commonly grade into each other [31].

3. Analytical methods

Samples used in this study are mainly harzburgite, dunite and chromitite of the two ophiolites with additional lherzolite from

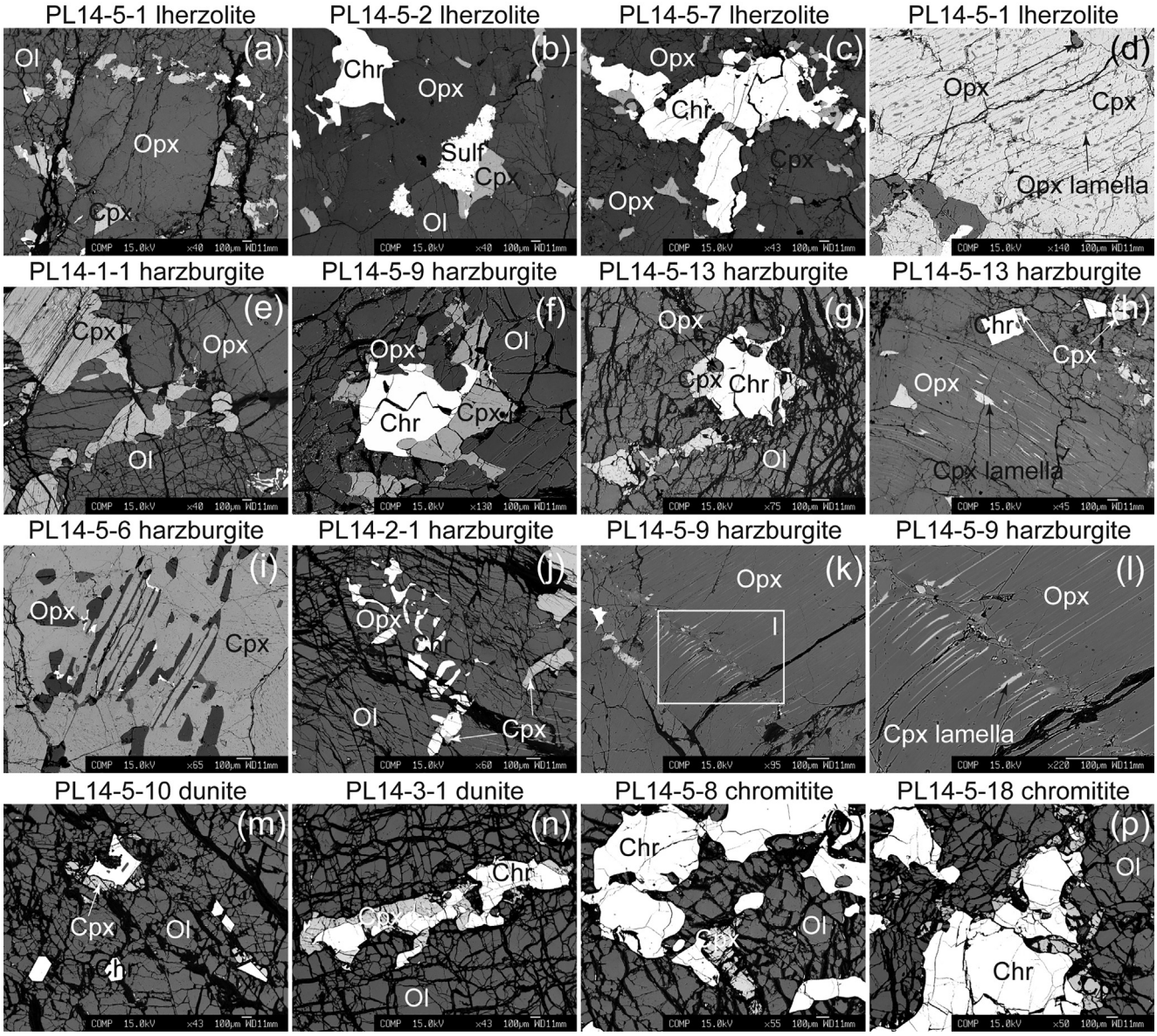

Fig. 3. (Color online) Back-scattered images of lherzolite (a–d), harzburgite (e–l), dunite (m, n) and chromitite (o, p) of the Purang ophiolite. See details in the main text. Chr, chromite; Cpx, clinopyroxene; Ol, olivine; Opx, orthopyroxene; Sulf, sulfide.

the Purang massif. In situ major and trace elements and back-scattered images of the olivine and chromite were obtained following microscope investigations. Average and representative data are shown in Tables S1 and S2 (online) and raw data are presented in Tables S3–S10 (online).

3.1. Major oxide analysis

Major element compositions of minerals were determined by wavelength dispersive spectrometry using a JEOL JXA8100 electron probe microanalyzer (EPMA) at the Institute of Geology and Geophysics, Chinese Academy of Sciences (IGGCAS), Beijing. The EPMA analyses were carried out at an accelerating voltage of 15 kV and 10 nA beam current, 5 μm beam spot and 10–30 s counting time on peak. Natural and synthetic minerals were used for standard calibration. A program based on the ZAF procedure was used for matrix corrections. Typical analytical accuracy for all of the elements analyzed is better than 1%–2%.

3.2. Trace element analysis

Trace element concentrations of olivine and chromite were determined with a 193 nm Coherent COMPex Pro ArF Excimer laser coupled to an Agilent 7500 a inductively coupled plasma mass spectrometer (LA-ICP-MS) at the IGGCAS. Before LA-ICP-MS analysis, thin sections previously coated with carbon for EPMA analyses were treated with 3% HNO_3, followed by de-ionized water and ethylene to clean the surfaces. Each analysis was performed using 80 μm-diameter ablating spots at 6 Hz with energy of ~100 mJ per pulse for 45 s after measuring the gas blank for 20 s. Standard reference materials NIST610 and NIST612 (GeoReM: http://georem.mpch-mainz.gwdg.de/) were used as external standards to produce calibration curves. Every eight analyses were followed by two analyses of the standards to correct for time-dependent drift. Calibration was performed using NIST612 as an external standard, together with Si and Mg as internal standard elements for olivine and chromite, respectively. Off-line data processing was performed using the GLITTER 4.0 program.

4. Results

4.1. Petrography and major oxide compositions of minerals

4.1.1. Purang ophiolite

The lherzolite and harzburgite of the Purang ophiolite have similar petrological features, mineral assemblages and mineral major oxide compositions, which have been widely documented in previous studies [29,49–51,69]. There are, however, some unique features that differentiate these lherzolites and harzburgites. In the lherzolites, clinopyroxene normally occurs as small, anhedral grains that occur as clusters or rims surrounding coarse-grained orthopyroxene (Fig. 3a). In most cases, the clinopyroxene is associated with chromite or rarely with sulfide (Fig. 3b, c). Orthopyroxene in the lherzolites not only occurs as large interstitial crystals but forms exsolution lamellae in the clinopyroxene. It can also occur as small grains in clinopyroxene-chromite clusters (Fig. 3c) and in large clinopyroxene crystals (Fig. 3d). A close association between clinopyroxene and orthopyroxene is also observed in the harzburgites (Fig. 3e–h). Orthopyroxene not only forms large crystals in the harzburgites but can also occur as inclusions within clinopyroxene (Fig. 3i) or embedded in clinoproxene-chromite clusters (Fig. 3j). Clinopyroxene lamellae are well developed in many orthopyroxene grains (Fig. 3h), particularly along cracks (Fig. 3k, l). Clinopyroxene is also present in many of the Purang dunites and chromitites, where it is commonly in contact with chromite [51] (Fig. 3m–p). Some chromite crystals contain silicate inclusions (Fig. 3m, o).

The major oxide mineral chemistry of the Purang lherzolites and harzburgites is very similar (Fig. S1 online). Olivine in the lherzolite and harzburgite has Fo (fosterite) contents of 90.5 to 92 and there is no apparent correlation with NiO contents (Fig. S1a online), whereas olivine in the dunites and chromitites has a slightly larger variation in Fo (90–93) and shows a positive correlation between Fo and NiO (Fig. S1b online).

All of the chromite grains analyzed in this study from the Purang chromitite are high-Al varieties with Cr# ($100 \times Cr/(Cr + Al)$) of <60, but sparse high-Cr varieties (Cr# > 60) have been reported in some harzburgite and dunite samples [53] (Fig. S1c online). Orthopyroxenes generally have variable CaO and Al_2O_3 contents and Cr#s and show weak or no correlation with Mg#s. Orthopyroxene lamellae in the clinopyroxene have lower Mg# and CaO and higher Al_2O_3 than the interstitial grains (Fig. S1d–f online).

Clinopyroxene compositions in the Purang samples are highly variable, and reflect the nature of the host. Although the Al_2O_3 contents and Mg#s of the clinopyroxene overlap each other in all types of rocks (Fig. S1g online), grains in the dunites and chromitites have higher CaO and Na_2O contents than those in the lherzolites and harzburgites (Fig. S1h, i online).

4.1.2. Luobusa ophiolite

The harzburgites, dunites and chromitites of the Luobusa ophiolite are somewhat more altered than those of the Purang massif. Primary textures are rare in the harzburgites and dunites, but are typically preserved in the chromitites and their associated lithologies. The least-altered samples were selected for chemical analysis, and their features and compositions can be representative by the sample in Fig. S2 (online), showing a transition from chromitite to dunite to harzburgite that is similar to the sample described in Zhou et al. [68] and Su et al. [30]. The harzburgites and some dunites typically contain trace amounts of clinopyroxene, whereas the chromitites normally consist of only olivine and chromite. Compositionally, the Luobusa harzburgites are more refractory than those of the Purang ophiolite; the silicate minerals have high Mg#s (e.g., olivine Fo up to 94) and the chromites have high Cr#s (up to 60) [30,68] (Fig. S2 online). Smooth compositional transitions from harzburgite to dunite and chromitite are thought to be due to melt-rock interaction [68], whereas abrupt changes between chromite and olivine bands in the chromitite are thought to be related to Fe-Mg exchange [30] (Fig. S2 online). The Luobusa dunites and chromitites have higher Fo values in olivine and higher Cr#s in chromite than those of the Purang ophiolite (Figs. S1b, c, S2 online).

4.2. Trace elements in olivine and chromite

In general, olivines in the Purang ophiolite have larger variations in trace element concentrations than those in the Luobusa massif (Figs. S3a, b (online) and 4); in contrast, the Purang chromites generally have narrow concentration ranges than those of Luobusa (Fig. S3c, d online). Variation trends of the trace elements in both olivine and chromite are significantly different between the two ophiolites and between rock types within each body (Fig. 4a, b), and thus, values for harzburgite and chromitite are plotted separately from dunite in Figs. 5 and 6.

4.2.1. Olivine

Olivine from lherzolites in Purang has Li (1.06–1.90 ppm), Sc (2.20–3.11 ppm), Ni (2,181–3,665 ppm) and Co (100–170 ppm) concentrations, typical for mantle olivine, which, together with the relatively high Fo (91–92), indicate a highly depleted origin. Concentrations of incompatible elements in olivine, e.g., P (mostly 6.31–11.1 ppm), Ca (116–216 ppm) and V (mostly 0.31–1.17 ppm) are below those of mantle olivine analyzed by Witt-Eickschen and O'Neill [70] (P: 20–160 ppm; Ca: 785–1,214 ppm; V: 12–76 ppm), which supports a depleted origin.

Olivine from harzburgites in Purang has trace element compositions similar to those in the lherzolites as follows; Li (1.24–2.24 ppm), Al (17.6–75.3 ppm), P (6.99–12.7 ppm), Ti (2.48–6.13 ppm), V (0.59–1.77 ppm), Mn (801–1,406 ppm), Co (96.6–179 ppm) and Zn (13.0–71.2 ppm), with high Sc (2.84–4.99 ppm), and highly variable Ca (66.5–257 ppm), Cr (5.70–190 ppm) and Ni (2,223–3,941 ppm) concentrations (Fig. S3a, b online). Some of the trace element compositions overlap with those in the olivine from the Luobusa harzburgites (e.g., P: 9.53–13.8 ppm; Ni: 3,144–3,807; V: 0.34–1.86 ppm), although the latter has overall higher Ti (4.99–8.39 ppm up to 22.7 ppm), lower Mn (826–1,092 ppm) and Zn (24.3–48.3 ppm), and moderate Sc (2.27–3.60 ppm) and Co (107–150 ppm).

Olivine in chromitites from the two ophiolites has distinctly different trace element contents. Those in the Purang chromitites are conspicuously rich in Al (16.3–17.9 ppm up to 82.9 ppm), Sc (2.85–7.50 ppm), V (0.28–2.43 ppm), Mn (1,103–1,370 ppm), Co (120–163 ppm), Zn (22.6–59.2 ppm), and poor in Ni (2,649–3,466 ppm). In contrast, olivine in the Luobusa chromitites has much lower concentrations (Al: 1.82–10.7 ppm; Sc: 2.43–2.82 ppm; V: 0.14–0.26 ppm; Mn: 563–656 ppm; Co: 69.2–91.9 ppm; Zn: 12.9–19.1 ppm) except for Ni (3,967–4,194 ppm). Dunites in both ophiolites have olivine with trace element compositions between those in harzburgite and chromitite in the individual ophiolites (Fig. S3a, b online).

4.2.2. Chromite

Chromite grains in the lherzolites and harzburgites of the Purang ophiolite have very similar trace element contents, which are generally lower than those in the Luobusa harzburgites (Fig. S3c, d online) such as Zn (382–1,946 ppm vs. 877–6,815 ppm), Ti (248–416 ppm vs. 378–1,285 ppm), and Mn (575–1,772 ppm vs. 942–9,416 ppm). The Luobusa harzburgites are also characterized by large variations in Si (575–7,263 ppm), Sc (1.01–4.56 ppm) and Cu (0.96–4,461 ppm).

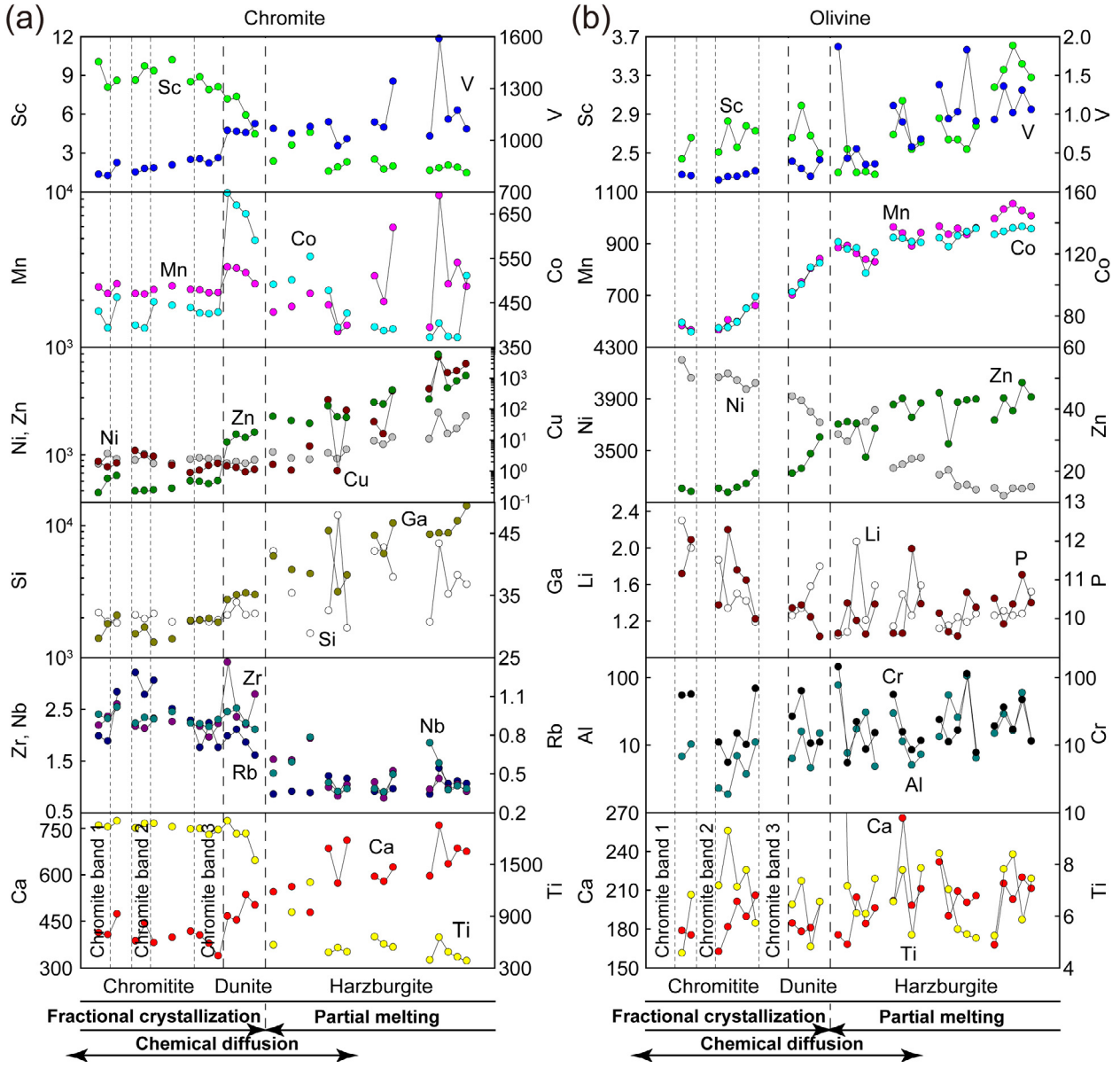

Fig. 4. Trace element (ppm) profiles of chromite (a) and olivine (b) in the transect harzburgite-dunite-chromitite sample from the Luobusa ophiolite as shown in Fig. S2 (online).

The Purang and Luobusa dunite samples have comparable Cu, Zn, Ca, Rb and Ga contents in chromite, but Ti, Co, Nb and Zr are more depleted in the former (Fig. S3c, d online). All samples show enrichment in Sc and Mn, and depletion in Ni compared to their corresponding lherzolite and/or harzburgite (Fig. 5e–j). Chromite compositions in the Purang dunites mostly overlap those of the coexisting chromitites, whereas in the Luobusa ophiolite chromite compositions of the dunites and chromitites are distinctly different (Figs. 4a and 6e–j).

The trace element data of chromite in the Luobusa chromitites obtained in this study are very similar to those reported by Zhou et al. [10], with additional elements, namely; Si (420–2,264 ppm), Ca (77.5–472 ppm), Rb (0.32–2.72 ppm), Zr (0.37–3.00 ppm) and Nb (0.18–2.53 ppm). They have basically higher Sc, Ti, Zr, Nb and Rb, and lower V, Ni, Zn, Si, Ca and Ga contents than those in the coexisting harzburgites and dunites (Fig. 4a).

5. Behaviors of trace elements of olivine and chromite under high-temperature processes

To date, the hypothesis of melt-peridotite interaction has been widely accepted to account for podiform chromite deposits in most ophiolites including Luobusa [5,6,15]. In this model, podiform chromitites are of magmatic origin and form from melts migrating through mantle peridotite. Dunite envelopes are the products of melt-rock reaction that strip the mantle residue of pyroxene and replace it with olivine in focused melt channels [21,71,72]. However, as seen in the chromitite-dunite-harzburgite transect described above, melt-rock reaction is a gradational process and the peridotites grade from harzburgite to dunite to chromitite [15,30,37,68] (Fig. S2 online). The harzburgites are considered to be residues of melt extraction as shown by their refractory mineral and bulk rock compositions, which later experienced chemical diffusion from the melts [30,68]. During melt-rock reaction both the

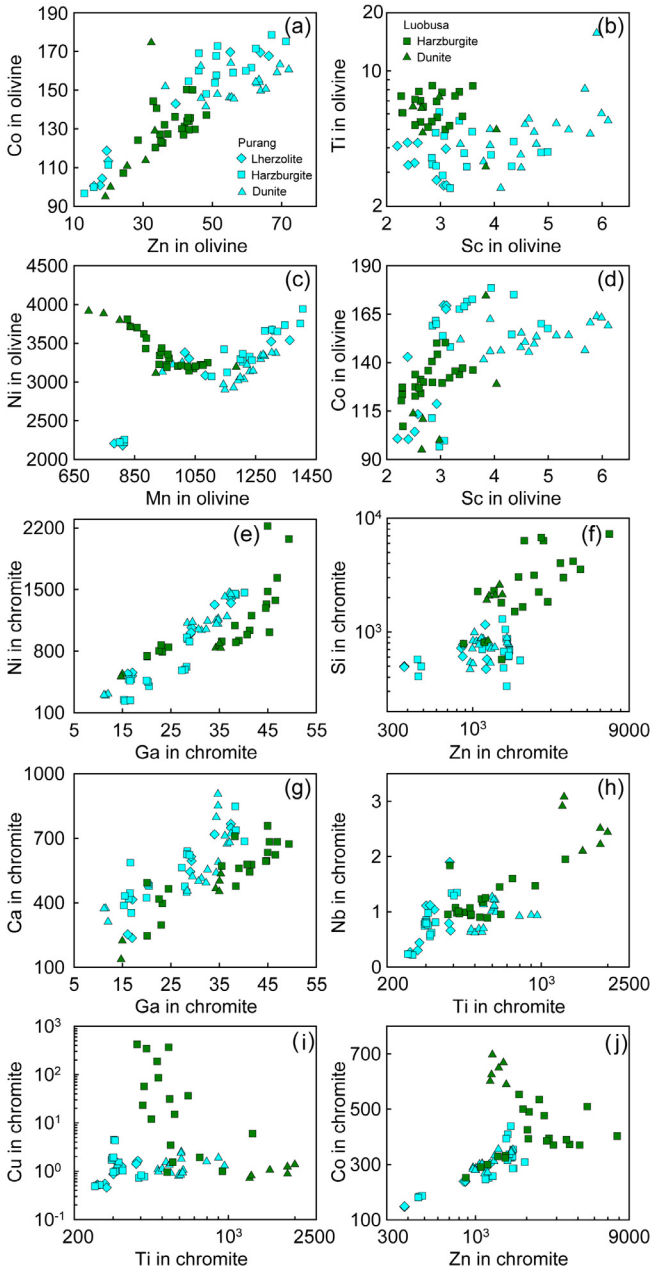

Fig. 5. Correlation diagrams of trace elements (ppm) for olivine (a–d) and chromite (e–j) in the harzburgite and dunite from the Purang and Luobusa ophiolites.

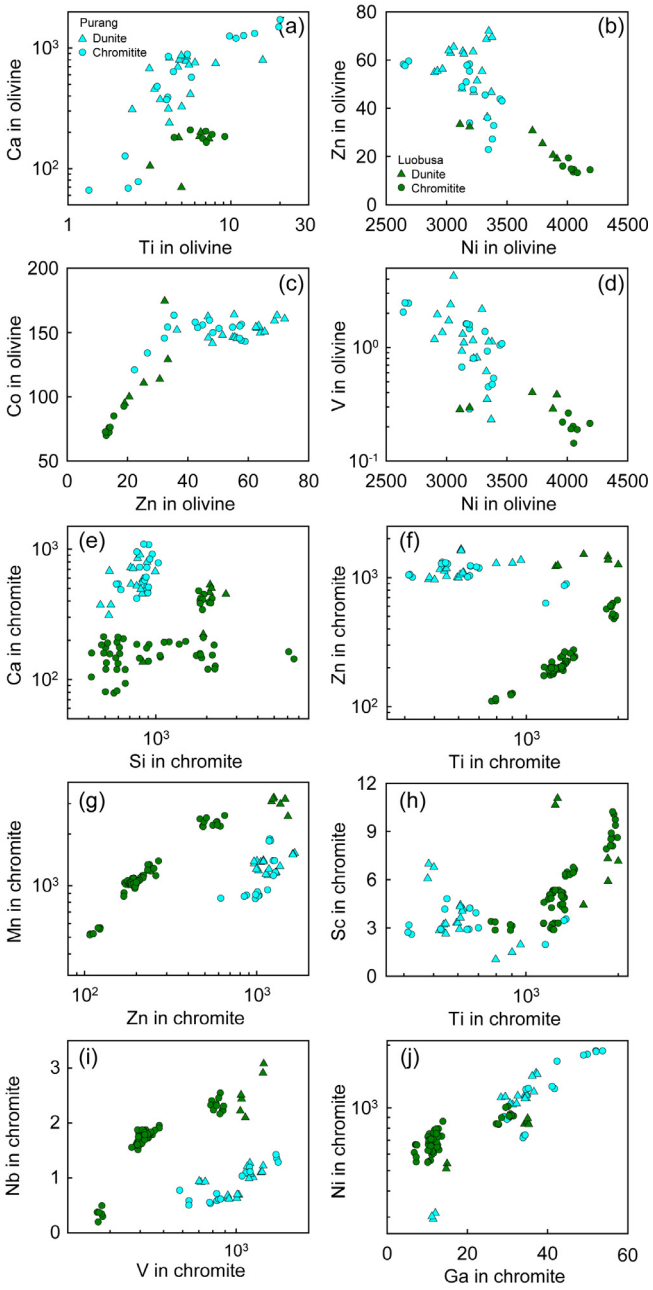

Fig. 6. Correlation diagrams of trace elements (ppm) for olivine (a–d) and chromite (e–j) in the dunite and chromitite from the Purang and Luobusa ophiolites.

Cr#s of chromite grains and the Fo values of olivine in the harzburgites are elevated [30] (Fig. S2 online). Clearly, dunite acts as a boundary between harzburgites and chromitites. In addition, subsolidus re-equilibration occurs between chromite and olivine within chromitites during cooling, further increasing the Fo content of the olivine [21,31].

Trace element analyses of chromite and olivine in the chromitite-dunite-harzburgite profile (Figs. S2 (online) and 4) from the Luobusa ophiolite record a complete range of processes of chromitite formation (partial melting of harzburgite, fractional crystallization of chromitite and dunite, reaction between melt and harzburgite and subsolidus diffusion between chromite and olivine) [30,68]. Thus, this profile provides an ideal opportunity to track the behaviors of trace elements in olivine and chromite during these high-temperature processes. Here we integrate our new data with findings of previous studies [5,10,21,32,37,73,74], to determine the behaviors of trace elements during the genesis and evolution of chromite deposits as well as ophiolites.

5.1. Partition coefficients of trace elements in chromite and olivine

Partition coefficients (D) of trace elements have been experimentally and empirically determined or estimated for chromite and olivine in basaltic and boninitic melts as displayed in https://earthref.org. This database shows that Co and Zn are highly compatible in chromite (D_{Co} = 2.1–8.3; D_{Zn} = 3.6–7.9), and that Ni, Cu and Ga are moderately compatible (D_{Ni} = 1.3–11; D_{Cu} = 3.1; D_{Ga} = 1.83–3.75). Elements such as Mn, Ti, and Sc are slightly to moderately incompatible in chromite with D values of 0.88–0.98, 0.05–0.75 and 0.18–0.57, respectively, whereas Rb, Zr and Nb are highly incompatible (D_{Rb} = 0.029; D_{Zr} = 0.03–0.14; D_{Nb} = 0.0006–

0.15). D_V values are highly variable (0.02 to 31), reflecting variations in oxygen fugacity [10,21,37]. Chromite in boninite has higher D_{Ti} and D_V values, similar D_{Sc} and D_{Mn} values, and lower D values of Co, Ni, Zn, Ga than those in MORB [21]. Although Si and Ca partition coefficients in chromite have not been determined, some experiments suggest that SiO_2 and CaO contents in chromite vary from a few thousands ppm to several percent depending on the ambient temperatures and pressures [75–78].

Because olivine is a major mineral phase in the mantle, its trace element variations have been well documented in various processes. Substitution of cations in olivine is more complex than in chromite due to its different crystal structure. In olivine, two elements, such as Al and Sc, or Li and P, are normally coupled to substitute for Mg and/or Si or to occupy vacancies to maintain charge balance [79–81]. Meanwhile, trivalent cations in olivine generally diffuse more slowly than divalent ones [33,37]. Co and Ni are both compatible in olivine with D values of 1.1–52 and 1.4–351, respectively (https://earthref.org), whereas elements such as Al, P, Ca and Ti have very low D values (<0.1) in olivine, and others including Li (D = 0.03–1.3) and Sc (D = 0.04–0.78) are moderately incompatible. Partition coefficients of V, Cr, Mn and Zn in olivine are highly variable from compatible to incompatible and appear to be susceptible to subsolidus reequilibration that is controlled not only by the temperature, but also by the distribution of the dominant divalent cations in coexisting chromite [17,33,34,73,82,83].

Subsolidus reequilibration, mainly Fe and Mg exchange, between chromite and olivine can significantly alter the elements that can diffuse in both minerals, rather than incompatible trace elements [33]. The intensity of the subsolidus reequilibration is a function of the relative proportion and composition of chromite and olivine [21,31,73,84], but the effect of subsolidus diffusion on the contents of many trace elements in chromite and olivine has not been well constrained.

However, major and trace elemental profiles of chromite and olivine in the Luobusa composite sample (Figs. S2 (online) and 4) clearly reveal the results of multiple high-temperature processes.

5.2. Behaviors of elements during partial melting

Compatible trace elements are thought to record primarily magmatic differentiation processes and their contents in residual mineral increase with the degree of partial melting, whereas incompatible elements can preserve signals of mantle-derived variability on both intra-and inter-eruption scales [36]. On the basis of major element variations of olivine and chromite (Fig. S2 online), the harzburgite portion displays decreasing degree of partial melting with distance away from its contact with dunite. Low but constant contents (<1.5 ppm) of Rb, Zr and Nb of chromite in harzburgite (Fig. 4a) indicate that they were mostly removed during partial melting and not altered by later processes because of their high incompatibility in chromite. Covariation of Sc and Ti agrees with their similar incompatibility, and their immediate increases close to the contact imply the possible influence by melt-harzburgite interaction. Manganese in the chromite displays similar content and trend as V (Fig. 4a), implying that Mn may also be dependent on oxygen fugacity [10,21,37]. The increasing trends of compatible elements such as Zn, Ni, Cu and Ga in chromite in the harzburgite with the distance away from the boundary with dunite, and the decoupling of olivine Fo values and chromite Cr#s (Figs. S2 (online) and 4a), suggest that these elements were controlled by both partial melting and melt diffusion. Chromite in these rocks contains high Si and Ca, and the absence of clear compositional trends of Si and Ca contents in chromite suggest that their contents may be primary features acquired when the chromite was initially formed.

Like chromite, olivines in the harzburgite (Fig. 4b) have low and generally constant abundances of incompatible elements, such as Li, P, Ca and Ti, whereas their Ni contents increase with increasing degrees of partial melting (Fig. 4b). The decrease of V and Sc contents of the olivines at the contact with dunite reflects possible diffusion into melts during melt-harzburgite interaction because V and Sc prefer more oxidized and melt phases [21,33]. Al and Cr show coupled variations, which are probably related to their reequilibration with the surrounding chromite and pyroxenes during partial melting. Covariations of Co, Mn and Zn contents suggest that they were moderately compatible elements during partial melting.

In summary, the concentrations and variations of most incompatible trace elements in the chromite and olivine in harzburgite mostly reflect varying degrees of partial melting, whereas the compatible trace element abundances depend on their partition coefficients between bulk peridotite and melt. Those elements such as Ni, which are compatible in both bulk rock samples and olivine and chromite, preserve partial melting signatures, whereas the other elements, which are compatible in olivine and chromite but incompatible in bulk rock, have been overprinted by a combination of partial melting and subsequent melt-harzburgite interaction.

5.3. Variation of elements during fractional crystallization and diffusion

The coupled variations of olivine Fo and FeO and chromite Mg# in the chromitite portion (Fig. S2 online) demonstrate significant Fe-Mg exchange between chromite and olivine. The intensity of Fe-Mg exchange is a function of the relative proportion of chromite and olivine such as, the higher the chromite proportion in the rock such as a chromite band (Fig. S2 online), the higher the modification of the olivine composition as revealed in previous studies [21,30,31]. Because of the high olivine/chromite ratios in dunites, the effects of Fe-Mg exchange can be ignored, at least for major elements. Smooth variation of chromite Cr# from chromitite to dunite is a typical feature of fractional crystallization [21,33,36].

Most trace elements in chromite in the chromitites display narrow compositional ranges and show no covariation trends with the major elements (Fig. 4a), suggesting that trace element compositions of the chromite are mainly related to parental magma compositions rather than magma differentiation. In contrast, coexisting olivines in the chromitite preserve good evidence of fractional crystallization such as systematical decreases in Mn, Co and Zn, and increases in Ni, Li and P with the increasing distance from the contact with the dunite (Fig. 4b). The overall lower Mn, Co and Zn contents in the olivine compared to their occurrence in the coexisting chromite (Fig. 4) indicate that their variations in olivine were dominantly controlled by co-crystallizing chromites preferentially incorporating these elements. Ni prefers to enter olivine rather than chromite during crystallization because D_{Ni} is higher in olivine [73,85], but elements such as Cr and Al preferentially enter chromite. Because chromite contains little or no Li [4,30] or P, the signatures of these two elements in olivine cannot be overprinted by elemental exchange with chromite and thus represent primary features.

In some cases, it is impossible to evaluate the effect of Fe-Mg exchange on the trace element compositions of olivine because olivine relicts in chromite bands are commonly too small to be analyzed using LA-ICP-MS. However, compositional comparisons of chromite between chromite bands and olivine bands point to slight enrichments in Mn, Co and Zn and depletions in Ni in chromite related to Fe-Mg exchange.

It is noteworthy that the trace element contents in the chromite show abrupt changes across the boundaries between harzburgite and dunite and between dunite and chromitite bands in the profile shown in Fig. 4a, whereas changes in olivine are gradual (Fig. 4b).

Crystallizing chromite appears to be more sensitive than olivine to the compositional changes of the magmas involved in melt-harzburgite interaction [5,6,15,30]. Thus, the chemical and physical changes of the interacting melt should have considerably modified partitioning coefficients of trace elements in chromite and introduced Si and Mg from pyroxene in the harzburgite to facilitate crystallization of voluminous olivine. Those elements in olivine that are not influenced by reequilibration with chromite, such as Cr, Al, Ti, Sc and V, show no correlations with the fractional crystallization trend, suggesting that they are controlled by coeval crystallization of chromite [21,73,82].

5.4. Mobilization of trace elements during serpentinization

It is known that serpentinization is a hydration reaction involving about 50% of solid volume increase [86]. This process produces a significant amount of hydrogen, which is related to magnetite formation from the Fe component in olivine [87–89]. In natural systems, the reaction stoichiometry and extent of volume change vary depending on the mechanism of element transport [90,91]. Thus, to understand element migration in ultramafic rocks it is important to consider serpentinization and its chemical and physical effects.

Serpentine in chromitite sample LBS13-01 from the Luobusa ophiolite has distinctive trace element compositions compared to pristine olivine in the same sample. Li depletion in serpentine (0.24–0.36 ppm) relative to olivine relicts (1.18–2.29 ppm) is interpreted to be related to preferential leaching of Li [4,92–94]. Valence-variable elements would presumably have been mobilized into serpentine due to an elevation in oxygen fugacity as shown by V (serpentine 1.07–2.38 ppm vs. olivine 0.14–0.26 ppm), Cr (serpentine 184–388 ppm vs. olivine 5.41–67.6 ppm), and Ti (serpentine 10.1–46.0 ppm vs. olivine 4.54–9.27 ppm). Elements having geochemical affinity with Fe, such as Mn, Co and Zn, preferentially entered magnetite, resulting in their depletion in serpentine (Mn 131–144 ppm; Co 11.1–15.9 ppm; Zn 4.97–5.10 ppm); whilst Sc and Ni were somewhat immobile during serpentinization as their contents lie between those of serpentine and olivine. The observed enrichments of Al, P and Ca in the serpentines are probably from the exotic reacting fluids.

6. Melt activities recorded in the Purang ophiolite

Melt penetration and melt-rock interaction following melt extraction have been documented in ophiolitic massifs worldwide [2,17,74,93,95], and the same processes have been suggested for the Luobusa and Purang ophiolites [4,47,51,65,96,97]. Intrusive pyroxenites and chromitites [51] (Fig. 2b, c), as well as mafic dykes with an age spectrum of 120–130 Ma [57,59], in the Purang peridotite massif indicate a long period of magmatic activity during its formation and evolution. Replacive dunites formed by melt-rock interaction are very similar to those in Luobusa [29,51,52], and metasomatism of the harzburgites is shown by the presence of plagioclase, amphibole and clinopyroxene [51,55,56,98]. These previous studies provide abundant elemental and isotopic data of minerals and whole-rock samples, but the genesis of the Purang lherzolites (melting residue vs. metasomatic product) and origin of the metasomatizing melts (MORB-like vs. arc magma) are still ambiguous.

6.1. Origin of pyroxenes and transformation from harzburgite to lherzolite

The lherzolite and harzburgite in the Purang ophiolite are very similar except for their modal abundance of clinopyroxene as described in Section 4.1. The occurrence of clinopyroxene surrounding orthopyroxene in both rock types [51] (Fig. 3a–c, e, h) indicates clinopyroxene precipitation at expense of orthopyroxene, which is further confirmed by the clinopyroxene-chromite association in all of the ophiolitic rocks (Fig. 3b, c, f, g, h, j, m–p) as discussed in Section 6.3. Enclosure of orthopyroxenes in clinopyroxene in some cases (Fig. 3c, d, f, g, i) suggests that the orthopyroxenes are incompletely transformed relicts. Morphological and chemical investigations have revealed that the clinopyroxenes in the Purang harzburgites are secondary and formed during melt-rock interaction [51,55,98]. Ca-enrichment of the percolating melts is inferred from anorthitic plagioclase [98], whereas the high-CaO olivine [51] in the Purang ophiolitic rocks reflects transformation from orthopyroxene to clinopyroxene. In addition, well-developed clinopyroxene lamellae in orthopyroxene of the harzburgites (Fig. 3h, k, l) further confirms the incorporation of clinopyroxene components into orthopyroxene, which could have been induced by interaction with melts [99].

Compositionally, both clinopyroxene and orthopyroxene in the Purang lherzolites plot within the ranges of their counterparts in the harzburgites (Fig. S1d–i online). Orthopyroxene relicts and lamellae in clinopyroxene and clinopyroxene lamellae in orthopyroxene also show nearly identical compositions to their corresponding interstitial grains. However, orthopyroxenes in the lherzolites are slightly enriched in Al_2O_3 and depleted in Cr_2O_3 compared to those in the harzburgites; likewise, the clinopyroxenes are enriched in Al_2O_3 and CaO and depleted in Na_2O at a given Mg# (Fig. S1e–i online). These petrological and mineralogical features point to the transformation of lherzolite from harzburgite via interaction with Ca- and Al-enriched and Cr- and Na-depleted melts. The random distribution of small lherzolite blocks in the huge harzburgite massif (Fig. 1c) shows that such interaction was localized.

In contrast, olivine and chromite from the lherzolites in Purang have restricted but generally higher Fo and Mg# ranges, respectively than those in the harzburgites (Fig. S1a, c online), suggesting that the major element compositions of the olivine and chromite were not significantly modified by melt-harzburgite interaction and maintain their primary residual nature. On the other hand, the trace elements of both olivine and chromite in the lherzolites and harzburgites apparently underwent kinetic diffusion from the metasomatic melts, as observed in the Luobusa ophiolite (Fig. S2 online), as demonstrated by their larger compositional variations (Fig. 5).

6.2. Metasomatic event for the dunite formation

In the Purang ophiolite the harzburgites contain numerous, small, lenticular to irregular bodies of dunite and lherzolite, although they are spatially separate (Fig. 1c). The dunites are commonly associated with bands of chromitite and have sharp contacts with the host harzburgite [49] (Fig. 2b, c), similar to those in the Luobusa ophiolite [68] (Fig. S2 online). Compositionally, the olivine and chromite in the dunites display larger and more variable Fo (90.5–93) and Cr# (35–80) values, respectively, than those of the lherzolites (Fig. S1b, c online). Clinopyroxenes in both the dunites and lherzolites are rich in CaO and Na_2O (Fig. S1h, i online). Likewise, both have the same contents and variations of compatible elements (Mn, Co, Ni, Zn) but the dunites and associated chromitites show significant enrichment in incompatible elements (e.g., Ca, Ti, Sc and P) (Fig. 5a–j). Both the physical and geochemical evidences suggest that the Purang dunites and lherzolites formed from two different metasomatic events, in which the harzburgites were invaded by compositionally distinctive melts. These two metasomatic agents are both relevant to chromite mineralization because chromitites in the Purang ophiolite are closely associated

with the lherzolites or dunites in the field [49,52,53] (Fig. 2b, c) and in the chemical plots (Fig. S1b, c, h, i online).

6.3. Metasomatic origin of clinopyroxene-chromite association

The clinopyroxene-chromite association as shown in Fig. 3 indicates their cogenetic origin. This association in the Purang lherzolites was previously interpreted to be symplectites formed by the breakdown of mantle garnet under spinel-facies conditions [51]. This conclusion was based on the similarity of these features to symplectites in orogenic peridotite massifs [100] and peridotite xenoliths [101]. The clinopyroxene-chromite association has been widely observed in various ophiolitic rocks, including harzburgite [102] (Fig. 3f–h, j), dunite [15,30,68,102] (Fig. 3m, n), chromitite [17,22,28,103] (Fig. 3o, p) and lherzolite [104] (Fig. 3b, c). Clinopyroxene compositions in these associations are comparable to those of interstitial and secondary counterparts in the same rock types (Fig. S1c, g–i online), suggesting their formation during melt-rock interaction. The high CaO and MgO and low Na_2O in these grains are very different from clinopyroxene in symplectites (low Ca and Mg and high Na) formed by the breakdown of mantle garnet [100,101,105]. Neither the high modal abundance of chromite in the ophiolite samples nor textures of these intergrowths (mostly clinopyroxene-enclosed chromite) (Fig. 3) are comparable to symplectite reported in orogenic peridotites and mantle peridotite xenoliths [101,105]. The occasional presence of orthopyroxene nuclei in the clinopyroxene-chromite association in the Purang lherzolites and harzburgites (Fig. 3c, f, g) implies incomplete interaction with the invading melts, and the absence of such orthopyroxene in the dunites and chromitites (Fig. 3m–p) suggests contemporaneous crystallization of clinopyroxene and chromite.

7. Relationship between melt activity and chromite mineralization

Many factors controlling the formation of economic chromite deposits in ophiolites have been proposed and these include physicochemical properties and compositions of migrating melts, melt replenishment, melt channels, refractory nature of host harzburgites, and tectonic environment [5,6,10,15,21,71,72]. The exact mechanism of chromite mineralization is, however, still ambiguous [9,11,39,102]. Here we compare the petrology and mineral chemistry of the mineralized Luobusa ophiolite and the barren Purang ophiolite in an attempt to shed new light on some aspects of chromitite formation.

7.1. Trace element comparisons between Luobusa and Purang ophiolites

7.1.1. Host harzburgite

Harzburgites in the Luobusa and the Purang ophiolites show large major oxide ranges of the major constituent minerals and overlap each other [15,29,30,51,55,68,96] (Figs. S1, S2 online). However, olivine and chromite in the harzburgites of these ophiolites have distinctly different trace elemental compositions and trends. Olivines in the Luobusa harzburgites generally show lower contents of most compatible trace elements (e.g., Co, Zn and Mn) but similar levels of most incompatible trace elements compared to olivines in the Purang samples (Fig. 5a, c), indicating higher levels of melt extraction in the Luobusa ophiolite than the Purang ophiolite. Contrasting correlation trends of Mn vs. Ni of the olivines in the two ophiolites (Fig. 5c) can be attributed to different diffusive behaviors of these two elements [82,106] and to the compositions of interacting melts as discussed in Section 5. This explanation also applies to higher Ti contents of the olivine in the Luobusa harzburgites (Fig. 5b).

Chromites display relatively large trace element differences between the Luobusa and the Purang harzburgites and generate well-defined correlations between the elements. The Luobusa chromites have much higher total trace element compositions compared to the Purang varieties (Fig. 5e–j). Enrichment of compatible trace elements (e.g., Ga, Zn, Cu and Co) in the Luobusa harzburgites is consistent with the resistance of chromite to partial melting [18,25]. The elevated incompatible trace element contents, such as Zr, Nb, Ti and Sc in the Luobusa chromite, are attributed to diffusion process from migrating melts (Fig. 4a). The significantly high contents (Fig. 5f) of pressure-dependant Si in the chromites [76–78] imply that the Luobusa harzburgites might have originated at a deeper depth than those of the Purang ophiolite.

Selected trace elements in olivine and chromite form good correlation trends in binary plots for the harzburgite and dunite from individual ophiolites. Some element pairs have similar trends on both ophiolites (Fig. 5a, d, e, f, h) but others do not (Fig. 5c, i, j), demonstrating the critical importance of migrating melt compositions and the geochemical behaviors of the trace elements. Secondary clinopyroxene may also account for some elemental anomalies (e.g., Ti in Fig. 5b, i) and the differences between the two ophiolites because it can accommodate larger volumes of trace elements than olivine and chromite. Melt-rock interaction resulted in more clinopyroxene crystallization in the Purang harzburgites than in Luobusa [51,55], even locally transforming harzburgite to lherzolite, which significantly decreased the distribution of some trace elements in and between chromite and olivine.

7.1.2. Dunite and chromitite

The close spatial association of dunite and chromitite in ophiolites is also mirrored in their mineral compositions; olivine and chromite in individual ophiolites plot in restricted fields and/or show linear correlations in binary trace element diagrams (Fig. 6). Olivines in the Purang dunites and chromitites are enriched in all compatible trace elements (except Ni) and some incompatible elements (Ca, V, Al and Sc) compared to samples from the Luobusa ophiolite. The two bodies show overlapping values of Li, Ti, Cr and P, and these two ophiolites show similar correlation trends. Relatively larger variations of trace element contents in the Purang olivines (Fig. 6a–d) are probably due to fewer analyses on the Luobusa olivines and the two metasomatic events in the Purang ophiolite (see Section 6). The associated chromites in the Purang ophiolite are enriched in Zn, Ca, V, Ni and Ga and depleted in Ti, Nb and Zr, and show narrow variations in Si, Sc, Mn, Co, Cu and Rb compared to samples from Luobusa. The Luobusa dunites and chromitites normally display good correlations between the trace elements of chromites, whereas the Purang chromites are mostly clustered with no clear co-variations in binary trace element diagrams (Fig. 6e–j).

Low Fo values of the olivines in the Purang dunites and chromitites (Fig. S1b online) indicate little or no Fe-Mg exchange between chromite and olivine unlike the extensive reequilibration observed in the Luobusa samples [15,30,31,96]. In summary, the Luobusa and the Purang ophiolites display rather contrasting trace element trends from the harzburgite to dunite and chromitite for both olivine and chromite (Fig. S3 online). These data suggest that the differences in trace element compositions between the Luobusa and Purang ophiolites were primarily controlled by the compositions of parental melts that interacted with the harzburgite accompanied by limited elemental diffusion.

7.1.3. Parental melts of chromitites and tectonic implications

Compilations of worldwide economic chromite deposits in ophiolites reveal that typical high-Cr and high-Al chromitites have

Cr# of >70 and <50, respectively. High-Cr varieties typically have <1,000 ppm Ni and <30 ppm Ga, whereas high-Al varieties have >1,100 ppm Ni, and >400 ppm Ga [10]. A few intermediate chromitites with Cr#s between 50 and 70 have been reported in a few ophiolites [17,28,74,95,107]. The disseminated, uneconomic chromitites of the Purang ophiolite span the full range of Cr#s from 20 to 60 (Fig. S1c online) and 52 to 89 in Xiong et al. [52], and have Ni contents of 700–1,100 ppm and Ga of 30–55 ppm (Fig. 6j).

Xiong et al. [52] attributed the sparse high-Cr type chromitites in the Purang ophiolite to percolation of bonititic melts in a supra-subduction zone environment on the basis of compositional similarities to typical high-Cr varieties in the Luobusa ophiolite [15,66]. The close spatial relationship of high-Al type chromitites with the lherzolites and dunites in Purang (Fig. 2b) and similarity in mineral compostions (Fig. S1c, g, h online) indicate formation from melts enriched in Al and Ca and depleted in Si and Na as well as highly incompatible trace elements like Nb and Zr. Such melts resemble many MORB-like melts proposed in the literature [29,51,55,59,98] but are assumed to have been more water-rich than typical MORB because of the presence of hydrous minerals (e.g., amphibole) as metasomatic products and insterstitial grains in lherzolite and chromitite [52,98]. Parental melts of the intermediate-Cr type chromitites in the Purang ophiolite, similar to those in the Guleman ophiolite, are inferred to lie compositionally between bonititic and MORB-like melts [74]. The penetration of these various types of melts should have occurred sequentially in the mantle section as evidenced by the continuous variations of mineral chemistry between the rocks from the Purang ophiolite (Fig. S3 online). Such compositional transitions from MORB-like to intermediate and boninitic melts correspond to lavas in modern Izu-Bonin-Mariana forearc, an area of subduction initiation [108–111]. By comparison, the Purang ophiolite probably formed in a forearc setting during the initial stage of the Neo-Tethyan ocean subduction. These aspects, combined with recent studies of associated mafic rocks that intrude the Purang peridotites [57–60], further support recently proposed rapid forearc exhumation of these peridotites during a period of about 10 Ma (120–130 Ma) [47,112].

7.2. Indications for the genesis and exploration of ophiolitic chromitites

Although extensive melt activities occurred in the Purang ophiolite, no economic chromite deposits were ever found in this massif. If the features of the Luobusa ophiolite are used as criteria for chromite mineralization, it would suggest that the Purang ophiolite has no potential. Compositional comparisons with the Luobusa ophiolites demonstrate several key points that may account for the barren nature of the Purang ophiolite.

7.2.1. Recycling crustal materials in parental melts

Recycling of both oceanic and continental crustal minerals has been documented in the Luobusa chromitites and peridotites [10,65,113–115]. Such recycling is compatible with the high contents of Nb, Zr and Ti in the chromites, because these elements are commonly enriched in crustal materials. These components are, in constrast, depleted in the Purang samples. Depleted Nd isotopes of clinopyroxenes in the Purang ophiolitic rocks [55] and normal mantle-like bulk Fe isotopes [29], together with MOR-like gabbros [29,54], further confirm smaller degrees of crustal contamination in the melts that percolated through the Purang peridotites. Thus, we conclude that involvement of recycled crustal materials in the parental melts is favorable to chromite crystallization and concentration [6,21]. Such a process is similar to the role of crustal assimilation in the formation of stratiform chromite deposits [116].

7.2.2. Refractory nature of mantle harzburgites

Chromium is a refractory and compatible element and is concentrated in highly refractory mantle rocks. The Cr content of crystallizing chromite can reflect the mantle source of the initial melts and the degree of melt-rock interaction [15]. Melt-harzburgite interaction is a process of remobilizing the element Cr via consumption of pyroxenes and reprecipitating it as chromite [6,117,118]. The refractory nature of the Luobusa harzburgites compared to those in Purang (e.g., chromite Cr# >45 vs. 20–60; Figs. S1c, S2 online) would facilitate increasing Cr concentration.

7.2.3. Crystallization of clinopyroxene and amphibole

Clinopyroxene is the secondmost Cr-rich mineral in the mantle. Widespread secondary clinopyroxene in the Purang peridotites and chromitites [52] (Fig. 3) was competing with chromite for Cr during crystallization of the melts. This competition was abetted by Ca-enrichment in the percolating melts, which favored transformation of orthopyroxene to clinopyroxene. This directly affected the concentration of Cr in the melt and hindered chromite crystallization. The presence of relict orthopyroxene in the clinopyroxene-chromite assemblages (Fig. 3c, d, f, g, i) indicates incomplete interaction probably due to low melt/rock ratios, and as a consequence, less Cr is released. Additionally, water/fluid plays an important role in chromite transportation and concentration [102,119] but it was mostly involved in the formation of amphibole and possibly clinopyroxene in the Purang ophiolite [52,98].

7.2.4. Significance of focussed melt channels

The significance of focussed melt channels has been highlighted in the formation of ophiolitic chromitite by many authors [9,13,15,71,72]. In the Purang ophiolite, there is abundant evidence of metasomatic minerals in all rock types (Fig. 3) and small chromitites are associated with lherzolites in the harzburgite massif (Fig. 1c). Thus, in Purang melt infiltration was relatively pervasive rather than being concentrated in focused melt channels, which hindered Cr concentration and the formation of large chromitite bodies.

7.2.5. Pressure and temperature conditions of chromitite formation

If the Si content in chromite is indeed dependant on pressure [76–78], the Luobusa mantle peridotites and chromitites should have formed at greater depths than those in the Purang ophiolite (Fig. 5f, 6e). Greater depths of formation are typically associated with higher temperatures. Efficient subsolidus exchange between chromite and olivine requires high initial temperatures of crystallization and long cooling times in relatively large melt chambers or channels [31,34,84]. Obviously, the insignificant subsolidus reequilibrium between chromite and olivine in the Purang dunites and chromitites suggests that they crystallized at a lower temperature and possibly experienced a faster uplift/emplacement than those in the Luobusa samples. This inference seems to be consistent with the tectonic settings in which the two ophiolites formed, that is, the Luobusa ophiolite was believed to have formed in a mature island arc [10,15,30], whereas the chromite deposit-barren Purang ophiolite formed during subduction initiation as discussed above.

Conflict of interest

The authors declare that they have no conflict of interest.

Acknowledgments

This work was supported by the National Natural Science Foundation of China (91755205 and 41772055), State Key Laboratory of Lithospheric Evolution (201701) and Youth Innova-

tion Promotion Association, Chinese Academy of Sciences (2016067).

Appendix A. Supplementary data

Supplementary data to this article can be found online at https://doi.org/10.1016/j.scib.2018.12.018.

References

[1] Pearce JA, Lippard SJ, Roberts S. Characteristics and tectonic significance of supra-subduction zone ophiolites. Geol Soc Lond Spec Publ 1984;16:77–94.
[2] Kelemen PB, Dick HJB, Quick JE. Formation of harzburgite by pervasive melt/rock reaction in the upper mantle. Nature 1992;358:635–41.
[3] Aitchison JC, Davis AM, Liu J, et al. Remnants of a Cretaceous intra-oceanic subduction system within the Yarlung-Zangbo suture (southern Tibet). Earth Planet Sci Lett 2000;183:231–44.
[4] Su BX, Chen C, Pang KN, et al. Melt penetration in oceanic lithosphere: Li isotope records from the Pozantı-Karsantı ophiolite in southern Turkey. J Petrol 2018;59:191–205.
[5] Arai S, Yurimoto H. Podiform chromitites of the Tari-Misaka ultramafic complex, Southwest Japan, as mantle-melt interaction products. Econ Geol 1994;89:1279–88.
[6] Zhou MF, Robinson PT, Bai WJ. Formation of podiform chromitites by melt/rock interaction in the upper mantle. Miner Deposit 1994;29:98–101.
[7] Zhou MF, Sun M, Keays RR, et al. Controls on the platinum-group elemental distributions in high-Cr and high-Al chromitites: a case study of the podiform chromitites from the Chinese orogenic belts. Geochim Cosmochim Acta 1998;62:677–88.
[8] Rollinson H. The geochemistry of mantle chromitites from the northern part of the Oman ophiolite: inferred parental melt compositions. Contrib Mineral Petrol 2008;156:273–88.
[9] Robinson PT, Zhou MF, Malpas J, et al. Podiform chromitites: their composition, origin and tectonic setting. Episodes 1997;20:247–52.
[10] Zhou MF, Robinson PT, Su BX, et al. Compositions of chromite, associated minerals, and parental magmas of podiform chromite deposits: the role of slab contamination of asthenospheric melts in suprasubduction zone environments. Gondwana Res 2014;26:262–83.
[11] Arai S, Miura M. Formation and modification of chromitites in the mantle. Lithos 2016;264:277–95.
[12] Thayer TP. Principal features and origin of podiform chromite deposits, and some observations on the Guleman-Soridag district, Turkey. Econ Geol 1964;59:1497–524.
[13] Thayer TP. Gravity differentiation and magmatic reemplacement of podiform chromite deposits. Eco Geol Monogr 1969;4:132–46.
[14] Dickey JS. Hypothesis of origin for podiform chromite deposits. Geochim Cosmochim Acta 1975;39:6–7.
[15] Zhou MF, Robinson PT, Malpas J, et al. Podiform chromitites in the Luobusa ophiolite (southern Tibet): implications for melt-rock interaction and chromite segregation in the upper mantle. J Petrol 1996;37:3–21.
[16] Su BX, Xiao Y, Chen C, et al. Potential applications of Fe and Mg isotopes in genesis of chromitite deposit in ophiolites. Earth Sci 2018;43:1011–24 (in Chinese).
[17] Chen C, Su BX, Xiao Y, et al. Intermediate chromitite in Kızıldağ ophiolite (SE Turkey) formed during subduction initiation in Neo-Tethys. Ore Geol Rev 2019;104:88–100.
[18] Barnes SJ, Roeder PL. The range of spinel compositions in terrestrial mafic and ultramafic rocks. J Petrol 2001;42:2279–302.
[19] Kamenetsky VS, Crawford AJ, Meffre S. Factors controlling chemistry of magmatic spinel: an empirical study of associated olivine, Cr-spinel and melt inclusions from primitive rocks. J Petrol 2001;42:655–71.
[20] Uysal İ, Sadiklar MB, Tarkian M, et al. Mineralogy and composition of the chromitites and their platinum-group minerals from Ortaca (Mugla-SW Turkey): evidence for ophiolitic chromitite genesis. Mineral Petrol 2005;83:219–42.
[21] Pagé P, Barnes SJ. Using trace elements in chromites to constrain the origin of podiform chromitites in the Thetford Mines ophiolite, Quebec, Canada. Econ Geol 2009;104:997–1018.
[22] Rollinson H, Adetunji J. The geochemistry and oxidation state of podiform chromitites from the mantle section of the Oman ophiolite: a review. Gondwana Res 2015;27:543–54.
[23] Dick HJB, Bullen T. Chromian spinel as a petrogenetic indicator in abyssal and alpine type peridotites and spatially associated lavas. Contrib Mineral Petrol 1984;86:54–76.
[24] Horn I, Foley SF, Jackson SE, et al. Experimentally determined partitioning of high-field strength and selected transition elements between spinel and basaltic melt. Chem Geol 1994;117:193–218.
[25] Irvine TN. Chromian spinel as a petrogenetic indicator: part I. Theory. Can J Earth Sci 1965;2:648–72.
[26] Baumgartner RJ, Zaccarini F, Garuti G, et al. Mineralogical and geochemical investigation of layered chromitites from the Bracco-Gabbro complex, Ligurian ophiolite, Italy. Contrib Mineral Petrol 2013;165:477–93.
[27] Evans KA, Powell R, Frost BR. Using equilibrium thermodynamics in the study of metasomatic alteration, illustrated by an application to serpentinites. Lithos 2013;168–169:67–84.
[28] Chen C, Su BX, Uysal İ, et al. Iron isotopic constraints on the origin of peridotite and chromitite in the Kizildag ophiolite, southern Turkey. Chem Geol 2015;417:115–24.
[29] Su BX, Teng FZ, Hu Y, et al. Iron and magnesium isotope fractionation in oceanic lithosphere and sub-arc mantle: perspectives from ophiolites. Earth Planet Sci Lett 2015;430:523–32.
[30] Su BX, Zhou MF, Robinson PT. Extremely large fractionation of Li isotopes in a chromitite-bearing mantle sequence. Sci Rep 2016;6:22370.
[31] Xiao Y, Teng FZ, Su BX, et al. Iron and magnesium isotopic constraints on the origin of chemical heterogeneity in podiform chromitite from the Luobusa ophiolite, Tibet. Geochem Geophys Geosyst 2016;17:940–53.
[32] Avcı E, Uysal İ, Akmaz RM, et al. Ophiolitic chromitites from the Kızılyüksek area of the Pozantı-Karsantı ophiolite (Adana, southern Turkey): implication for crystallization from a fractionated boninitic melt. Ore Geol Rev 2017;90:166–83.
[33] Spandler C, O'Neill HS, Kamenetsky VS. Survival times of anomalous melt inclusions from element diffusion in olivine and chromite. Nature 2007;447:303–6.
[34] Bai Y, Su BX, Xiao Y, et al. Origin of reverse zoned Cr-spinels from the Paleoproterozoic Yanmenguan mafic-ultramafic complex in the North China Craton. Minerals 2018;8:62.
[35] Le Roux V, Dasgupta R, Lee CT. Mineralogical heterogeneities in the Earth's mantle: constraints from Mn Co, Ni and Zn partitioning during partial melting. Earth Planet Sci Lett 2011;307:395–408.
[36] Neave DA, Shorttle O, Oeser M, et al. Mantle-derived trace element variability in olivines and their melt inclusions. Earth Planet Sci Lett 2018;483:90–104.
[37] Dare SAS, Pearce JA, McDonald I, et al. Tectonic discrimination of peridotites using fO_2-Cr# and Ga-Ti-Fe^{III} systematic in chrome-spinel. Chem Geol 2009;261:199–216.
[38] González-Jiménez JM, Augé T, Gervilla F, et al. Mineralogy and geochemistry of platinum-rich chromitites from the mantle-crust transition zone at Ouen Island, New Caledonia ophiolite. Can Mineral 2011;49:1549–70.
[39] González-Jiménez JM, Griffin WL, Proenza JA, et al. Chromitites in ophiolites: how, where, when, why? Part II. The crystallization of chromitites. Lithos 2014;189:140–58.
[40] Aldanmaz E. Trace element geochemistry of primary mantle minerals in spinel-peridotites from polygenetic MOR-SSZ suites of SW Turkey: constraints from an LA-ICP-MS study and implications for mantle metasomatism. Geol J 2012;47:59–76.
[41] Akmaz RM, Uysal İ, Saka S. Compositional variations of chromite and solid inclusions in ophiolitic chromitites from the southeastern Turkey: implications for chromitite genesis. Ore Geol Rev 2014;58:208–24.
[42] Colás V, González-Jiménez JM, Griffin WL, et al. Fingerprints of metamorphism in chromite: new insights from minor and trace elements. Chem Geol 2014;389:137–52.
[43] Colás V, Padrón-Navarta JA, González-Jiménez JM, et al. Compositional effects on the solubility of minor and trace elements in oxide spinel minerals: insights from crystal-crystal partition coefficients in chromite exsolution. Am Mineral 2016;101:1360–72.
[44] Yin A, Harrison TM. Geologic evolution of the Himalayan-Tibetan orogen. Annu Rev Earth Planet Sci 2000;28:211–80.
[45] Malpas J, Zhou MF, Robinson PT, et al. Geochemical and geochronological constraints on the origin and emplacement of the Yarlung Zangbo ophiolites, southern Tibet. Geol Soc Lond Spec Publ 2004;218:191–206.
[46] Hébert R, Bezard R, Guilmette C, et al. The Indus-Yarlung Zangbo ophiolites from Nanga Parbat to Namche Barwa syntaxes, southern Tibet: first synthesis of petrology, geochemistry, and geochronology with incidences on geodynamic reconstructions of Neo-Tethys. Gondwana Res 2012;22:377–97.
[47] Xiong FH, Yang JS, Robinson PT, et al. Diamonds and other exotic minerals recovered from peridotites of the Dangqiong ophiolite, western Yarlung-Zangbo suture zone, Tibet. Acta Geol Sin 2016;90:425–39.
[48] He L, Chen L, Dorji, et al. Mapping chromite deposits with audio magnetotellurics in the Luobusa ophiolite of southern Tibet. Geophysics 2018;83:47–57.
[49] Xu XZ, Yang JS, Guo GL, et al. Lithological research on the Purang mantle peridotite in western Yarlung-Zangbo suture zone in Tibet. Acta Petrol Sin 2011;27:3179–96 (in Chinese).
[50] Guo G, Yang J, Liu X, et al. Mid-ocean ridge (MOR) and suprasubduction zone (SSZ) geological events in the Yarlung Zangbo suture zone: evidence from the mineral record of mantle peridotites. J Asian Earth Sci 2015;110:33–54.
[51] Gong XH, Shi RD, Griffin WL, et al. Recycling of ancient subduction-modified mantle domains in the Purang ophiolite (southwestern Tibet). Lithos 2016;262:11–26.
[52] Xiong FH, Yang JS, Liu Z, et al. High-Cr and high-Al chromitite found in western Yarlung-Zangbo suture zone in Tibet. Acta Petrol Sin 2013;29:1878–908 (in Chinese).
[53] Xiong FH, Yang JS, Xu XZ, et al. Compositional and isotopic heterogeneities in the Neo-Tethyan upper mantle recorded by coexisting Al-rich and Cr-rich chromitites in the Purang peridotite massif, SW Tibet (China). J Asian Earth Sci 2018;159:109–29.

[54] Liu F, Yang JS, Dilek Y, et al. Geochronology and geochemistry of basaltic lavas in the Dongbo and Purang ophiolites of the Yarlung-Zangbo Suture zone: plume-influenced continental margin-type oceanic lithosphere in southern Tibet. Gondwana Res 2015;27:701–18.
[55] Miller C, Thöni M, Frank W, et al. Geochemistry and tectonomagmatic affinity of the Yungbwa ophiolite, SW Tibet. Lithos 2003;66:155–72.
[56] Liu CZ, Zhang C, Yang LY, et al. Formation of gabbronorites in the Purang ophiolite (SW Tibet) through melting of hydrothermally altered mantle along a detachment fault. Lithos 2014;205:127–41.
[57] Li J, Xia B, Liu L, et al. SHRIMP U-Pb dating of dolerite in the La'nga Co ophiolite, Burang, Tibet, China, and its geological significance. Geol Bull China 2008;27:1739–43 (in Chinese).
[58] Xia B, Li JF, Xu L, et al. Sensitive high resolution ion microprobe U-Pb zircon geochronology and geochemistry of mafic rocks from the Pulan-Xiangquanhe ophiolite, Tibet: constraints on the evolution of the Neo-Tethys. Acta Geol Sin 2011;85:840–53.
[59] Liu Z, Li Y, Xiong FH, et al. Petrology and geochronology of MOR gabbro in the Purang ophiolite of western Tibet, China. Acta Petrol Sin 2011;27:3269–79 (in Chinese).
[60] Chan GHN, Aitchison JC, Crowley QG, et al. U-Pb zircon ages for Yarlung Tsangpo suture zone ophiolites, southwestern Tibet and their tectonic implications. Gondwana Res 2015;27:719–32.
[61] Zhou S, Mo XX, Mahoney JJ, et al. The Pb-Nd isotope and Sm-Nd ages characteristics of diabase and gabbros in Lobusha area, Tibet. Chin Sci Bull 2001;46:1387–90 (in Chinese).
[62] Zhong LF, Xia B, Zhang YQ, et al. SHRIMP age determination of the diabase in Luobusa ophiolite, southern Xizang (Tibet). Geol Rev 2006;52:224–9 (in Chinese).
[63] Zhang C, Liu CZ, Wu FY, et al. Geochemistry and geochronology of mafic rocks from the Luobusa ophiolite, south Tibet. Lithos 2016;245:93–108.
[64] Bai WJ, Zhou MF, Robinson PT. Possible diamond-bearing mantle peridotites and chromitites in the Luobusa and Dongqiao ophiolites, Tibet. Can J Earth Sci 1993;30:1650–9.
[65] Shi R, Alard O, Zhi X, et al. Multiple events in the Neo-Tethyan oceanic upper mantle: evidence from Ru-Os-Ir alloys in the Luobusa and Dongqiao ophiolitic podiform chromitites, Tibet. Earth Planet Sci Lett 2007;261:33–48.
[66] Zhou MF, Robinson PT. Origin and tectonic environment of podiform chromite deposits. Econ Geol 1997;92:259–62.
[67] Li ZJ. Prospecting for the Chromite Ores in the Luobusa Ophiolite, Tibet. Wuhan: China University of Geoscienccs Press; 1993. p. 166 (in Chinese).
[68] Zhou MF, Robinson PT, Malpas J, et al. REE and PGE geochemical constraints on the formation of dunites in the Luobusa ophiolite, southern Tibet. J Petrol 2005;46:615–39.
[69] Li XP, Chen HK, Wang ZL, et al. Spinel peridotite, olivine websterite and the textural evolution of the Purang ophiolite complex, western Tibet. J Asian Earth Sci 2015;110:55–71.
[70] Witt-Eickschen G, O'Neill HSC. The effect of temperature on the equilibrium distribution of trace elements between clinopyroxene, orthopyroxene, olivine and spinel in upper mantle peridotite. Chem Geol 2005;221:65–101.
[71] Kelemen PB, Whitehead JA, Aharonov E, et al. Experiments on flow focusing in soluble porous media, with applications to melt extraction from the mantle. J Geophys Res 1995;100:475–96.
[72] Kelemen PB, Hirth G, Shimizu N, et al. A review of melt migration processes in the adiabatically upwelling mantle beneath oceanic spreading ridges. Philos Trans R Soc Lond 1997;355:283–318.
[73] Paktunc AD, Cabri LJ. A proton- and electron-microprobe study of gallium, nickel and zinc distribution in chromian spinel. Lithos 1995;35:261–82.
[74] Uysal İ, Kapsiotis A, Akmaz RM, et al. The Guleman ophiolitic chromitites (SE Turkey) and their link to a compositionally evolving mantle source during subduction initiation. Ore Geol Rev 2018;93:98–113.
[75] Gasparik T. Orthopyroxene thermobarometry in simple and complex systems. Contrib Mineral Petrol 1987;96:357–70.
[76] Liu X, O'Neill HSC. Partial melting of spinel lherzolite in the system CaO-MgO-Al_2O_3-SiO_2±K_2O at 1.1 GPa. J Petrol 2004;45:1339–68.
[77] Wu Y, Xu MJ, Jin ZM, et al. Experimental constraints on the formation of the Tibetan podiform chromitites. Lithos 2016;245:109–17.
[78] Zhang YF, Jin ZM, Griffin WL, et al. High-pressure experiments provide insights into the Mantle Transition Zone history of chromitite in Tibetan ophiolites. Earth Planet Sci Lett 2017;463:151–8.
[79] Nielsen RL, Gallahan WE, Newberger F. Experimentally determined mineral-melt partition coefficients for Sc, Y, REE for olivine, orthopyroxene, pigeonite, magnetite and ilmenite. Contrib Mineral Petrol 1992;110:488–99.
[80] Seitz HM, Woodland AB. The distribution of lithium in peridotitic and pyroxenitic mantle lithologies – an indicator of magmatic and metasomatic processes. Chem Geol 2000;166:47–64.
[81] Mallmann G, O'Neill HSC, Klemme S. Heterogeneous distribution of phosphorus in olivine from otherwise well-equilibrated spinel peridotite xenoliths and its implications for the mantle geochemistry of lithium. Contrib Mineral Petrol 2009;158:485–504.
[82] Qian Q, O'Neill HSC, Hermann J. Comparative diffusion coefficients of major and trace elements in olivine at ~950 °C from a xenocryst included in dioritic magma. Geology 2010;38:331–4.
[83] Bai Y, Su BX, Chen C, et al. Base metal mineral segregation and Fe-Mg exchange inducing extreme compositions of olivine and chromite from the Xiadong Alaskan-type complex in the southern part of the Central Asian Orogenic Belt. Ore Geol Rev 2017;90:184–92.
[84] Melcher F, Grum W, Simon G, et al. Petrogenesis of the ophiolitic giant chromite deposits of Kempirsai, Kazakhstan: a study of solid and fluid inclusions in chromite. J Petrol 1997;38:1419–58.
[85] Stosch HG. Sc, Cr, Co and Ni partitioning between minerals from spinel peridotite xenoliths. Contrib Mineral Petrol 1981;78:166–74.
[86] Coleman RG, Keith TE. A chemical study of serpentinization—Burro Mountain, California. J Petrol 1971;12:311–28.
[87] McCollom TM, Bach W. Thermodynamic constraints on hydrogen generation during serpentinization of ultramafic rocks. Geochim Cosmochim Acta 2009;73:856–75.
[88] Frisby C, Bizimis M, Mallick S. Seawater-derived rare earth element addition to abyssal peridotites during serpentinization. Lithos 2016;248–251:432–54.
[89] Shimizu H, Okamoto A. The roles of fluid transport and surface reaction in reaction-induced fracturing, with implications for the development of mesh textures in serpentinites. Contrib Mineral Petrol 2016;171:1–18.
[90] Okamoto A, Ogasawara Y, Ogawa Y, et al. Progress of hydration reactions in olivine-H_2O and orthopyroxenite-H_2O systems at 250 °C and vapor-saturated pressure. Chem Geol 2011;289:245–55.
[91] Malvoisin B. Mass transfer in the oceanic lithosphere: serpentinization is not isochemical. Earth Planet Sci Lett 2015;430:75–85.
[92] Decitre SE, Deloule E, Reisberg L, et al. Behavior of Li and its isotopes during serpentinization of oceanic peridotites. Geochem Geophys Geosyst 2002;3:1–20.
[93] Lundstrom CC, Chaussidon M, Hsui AT, et al. Observations of Li isotopic variations in the Trinity Ophiolite: evidence for isotopic fractionation by diffusion during mantle melting. Geochim Cosmochim Acta 2005;69:735–51.
[94] Vils F, Pelletier L, Kalt A, et al. The lithium, boron and beryllium content of serpentinized peridotites from ODP Leg 209 (Sites 1272A and 1274A): implications for lithium and boron budgets of oceanic lithosphere. Geochim Cosmochim Acta 2008;72:5475–504.
[95] Chen C, Su BX, Jing JJ, et al. Geological records of subduction initiation of Neo-Tethyan ocean: ophiolites and metamorphic soles in southern Turkey. Acta Petrol Sin 2018;34:3302–14 (in Chinese).
[96] Xiong FH, Yang JS, Robinson PT, et al. Origin of podiform chromitite, a new model based on the Luobusa ophiolite, Tibet. Gondwana Res 2015;27:525–42.
[97] Xiong F, Yang J, Robinson PT, et al. High-Al and high-Cr podiform chromitites from the western Yarlung-Zangbo suture zone, Tibet: implications from mineralogy and geochemistry of chromian spinel, and platinum-group elements. Ore Geol Rev 2017;80:1020–41.
[98] Liu CZ, Wu FY, Wilde SA, et al. Anorthitic plagioclase and pargasitic amphibole in mantle peridotites from the Yungbwa ophiolite (southwestern Tibetan Plateau) formed by hydrous melt metasomatism. Lithos 2010;114:413–22.
[99] Liang Z, Xiao Y, Thakurta J, et al. Exsolution lamellae in olivine grains of dunite units from different types of mafic-ultramafic complexes. Acta Geol Sin 2018;92:586–99.
[100] Marchesi C, Garrido CJ, Bosch D, et al. Mantle refertilization by melts of crustal-derived garnet pyroxenite: evidence from the Ronda peridotite massif, southern Spain. Earth Planet Sci Lett 2013;362:66–75.
[101] Shimizu Y, Arai S, Morishita T, et al. Origin and significance of spinel-pyroxene symplectite in lherzolite xenoliths from Tallante, SE Spain. Mineral Petrol 2008;94:27–43.
[102] Johan Z, Martin RF, Ettler V. Fluids are bound to be involved in the formation of ophiolitic chromite deposits. Eur J Mineral 2017;29:543–55.
[103] Lenaz D, Adetunji J, Rollinson H. Determination of $Fe^{3+}/\Sigma Fe$ ratios in chrome spinels using a combined Mössbauer and single-crystal X-ray approach: application to chromitites from the mantle section of the Oman ophiolite. Contrib Mineral Petrol 2014;167:1–17.
[104] Saka S, Uysal İ, Akmaz RM, et al. The effects of partial melting, melt-mantle interaction and fractionation on ophiolite generation: constraints from the late Cretaceous Pozantı-Karsantı ophiolite, southern Turkey. Lithos 2014;202:300–16.
[105] Su BX, Zhang HF, Wang QY, et al. Spinel-garnet phase transition zone of Cenozoic lithospheric mantle beneath the eastern China and western Qinling and its T-P condition. Acta Petrol Sin 2007;23:1313–20 (in Chinese).
[106] Spandler C, O'Neill HSC. Diffusion and partition coefficients of minor and trace elements in San Carlos olivine at 1300 °C with some geochemical implications. Contrib Mineral Petrol 2010;159:791–818.
[107] Lan CL, He SL, Li JL. Tectonic settings and metallogenic mechanism of ophiolitic chromites. J Gansu Sci 2006;18:53–6 (in Chinese).
[108] Stern RJ, Bloomer SH. Subduction zone infancy: examples from the Eocene Izu-Bonin-Mariana and Jurassic California arcs. Geol Soc Am Bull 1992;104:1621–36.
[109] Stern RJ, Reagan M, Ishizuka O, et al. To understand subduction initiation, study forearc crust: to understand forearc crust, study ophiolites. Lithosphere 2012;6:469–83.
[110] Reagan MK, Ishizuka O, Stern RJ, et al. Fore-arc basalts and subduction initiation in the Izu-Bonin-Mariana system. Geochem Geophys Geosyst 2010;11:Q03X12.
[111] Morishita T, Tani K, Shukuno H, et al. Diversity of melt conduits in the Izu-Bonin-Mariana forearc mantle: implications for the earliest stage of arc magmatism. Geology 2011;39:411–4.

[112] Maffione M, van Hinsbergen DJJ, Koornneef LMT, et al. Forearc hyperextension dismembered the south Tibetan ophiolites. Geology 2015;43:475–8.
[113] Yang JS, Dobrzhinetskaya L, Bai WJ, et al. Diamond- and coesite-bearing chromitites from the Luobusa ophiolite, Tibet. Geology 2007;35:875–8.
[114] Yang JS, Zhang ZM, Li TF. Unusual minerals from harzburgite, the host rock of the Luobusa chromite deposit, Tibet. Acta Petrol Sin 2008;24:1445–52 (in Chinese).
[115] Yamamoto S, Komiya T, Hirose K, et al. Coesite and clinopyroxene exsolution lamellae in chromites: in-situ ultrahigh-pressure evidence from podiform chromitites in the Luobusa ophiolite, southern Tibet. Lithos 2009;109:314–22.
[116] Irvine TN. Origin of chromite layers in the Muskox intrusion and other intrusions: a new interpretation. Geology 1977;5:273–7.
[117] Kelemen PB, Dick HJB. Focused melt flow and localized deformation in the upper mantle: juxtaposition of replacive dunite and ductile shear zones in the Josephine peridotite, SW Oregon. J Geophys Res 1995;100:423–38.
[118] Arai S. Control of wall-rock composition on the formation of podiform chromitites as a result of magma/peridotite interaction. Resour Geol 1997;47:177–87.
[119] Matveev S, Ballhaus C. Role of water in the origin of podiform chromitite deposits. Earth Planet Sci Lett 2002;203:235–43.

Benxun Su is a professor at the Institute of Geology and Geophysics, Chinese Academy of Sciences. His research interests focus on petrogenesis and mineralization of mafic-ultramafic rocks including mantle xenoliths, ophiolites, mafic-ultramafic intrusions and associated Cr-Ni-Cu-PGE deposits. He also works on Li-O isotope standard development for in situ analyses on SIMS and LA-MC-ICP-MS and applications in high temperature processes.